Surface profile analysis using a fiber-optic low-coherence interferometer

Robert Schmitt[a], Niels König[a] and Elisa Manfrin de Araújo[a,b]

[a]Fraunhofer Institute for Production Technology IPT
Steinbachstrasse 17, 52074 Aachen, Germany;
[b]Universidade Federal de Santa Catarina (UFSC), Brasil

ABSTRACT

Several optical measurement principles have proven their potential for high-resolution surface measurements. Among a few others, white-light interferometry has proven its capability for the measurement of technical surfaces, but yet, white-light interferometer systems cannot be miniaturized enough e.g. for the measurement inside small boreholes.
In this work, a fiber-optic measurement system is described. Since the measuring principle is based on low-coherence interferometry (LCI), the system provides non-contact surface measurements with nanometer accuracy. We present a system set-up for surface profile acquisition as well as the application of the system for the determination of roughness and waviness parameters. An outstanding feature of the proposed system is the miniaturized fiber-optic sensing probe, which is built up in all-fiber design. With a probe diameter down to 800 µm, the system can be used for measurements inside small cavities, e.g. bearings or injection nozzles. Beam shaping is realized with graded-index (GRIN) fibers. Conclusively, the results of evaluation measurements are compared with ISO 5436-1 type A and D measurement standards.

Keywords: low-coherence interferometry, surface profile, roughness, waviness, fiber-optic sensors

1. INTRODUCTION

The increasing possibilities of modern production technologies enable the manufacturing of high-tech products under extremly efficient conditions in terms of production time, cost and quality. Ultra-precision technology with diamond tools for example is capable of manufacturing of molds for mass replication of optics.[1] Customized free-form surfaces can be machined with optical quality.[2] Since production metrology is an enabling factor for the continuity of this trend, measurement systems have to keep up in terms of accuracy and speed. Ideally, a measurement system has to be suited for a machine integration to provide inline or even in-process measurement data. This way, machining imprecisions due to mounting and dismounting of the workpiece can be avoided.

For the characterization of surface profiles tactile stylus systems are still state of the art and provide highly accurate profile measurements with nanometer resolution. Additionally, tactile roughness measurements are comprehensively standardized by the international Geometric Product Specification (GPS) standards. However, tactile probing is often prohibited because of the possible deformation or damage of the surface. Furthermore, tactile measurement systems operate too slow for in-process measurements. Non-contact, optical measuring methods such as white-light interferometry,[3] confocal microscopy[4] or fringe projection[5] have proven to be feasible for non-destructive surface inspection. Nevertheless, for some measuring tasks, such as measurements in small spaces e.g. boreholes, most tactile and optical measurement systems cannot be miniaturized enough.

Within this work, a fiber-optic system for surface profile analysis will be described. Since the measuring principle is based on low-coherence interferometry, the system enables measurements even on rough surfaces. The sensor tip is realized in all-fiber design, thus the miniaturization of the sensor head enables measurements within limited spaces. The results of a series of evaluation measurements on miscellaneous calibration standards will be presented, which prove the suitability of the described system for surface profile analysis.

Further author information: (Send correspondence to N. König)
R. Schmitt: E-mail: robert.schmitt@ipt.fraunhofer.de, Telephone: +49 (0)241 8904-108
N. König: E-mail: niels.koenig@ipt.fraunhofer.de, Telephone: +49 (0)241 8904-113
E. Manfrin de Araújo: E-mail: elisamanfrin@gmail.com

Optical Measurement Systems for Industrial Inspection VI, edited by Peter H. Lehmann, Proc. of SPIE
Vol. 7389, 738914 · © 2009 SPIE · CCC code: 0277-786X/09/$18 · doi: 10.1117/12.827823

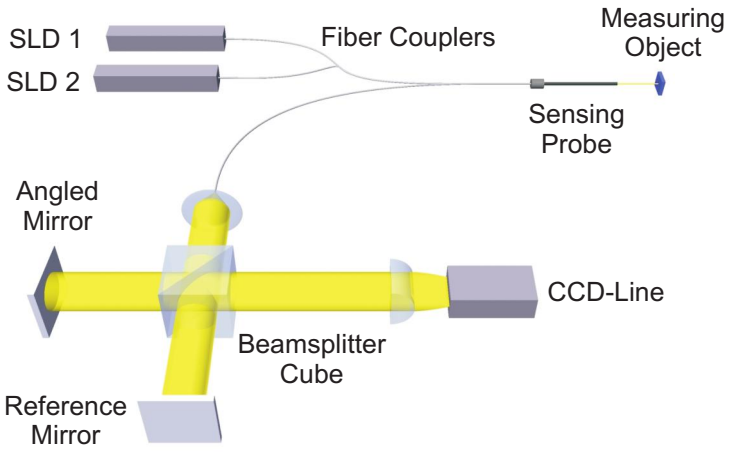

Figure 1. System set-up

2. FIBER-OPTIC LOW-COHERENCE INTERFEROMETER

2.1 System set-up

As shown in Fig. 1, the system set-up mainly comprehends two units: the sensing probe and the low-coherence interferometer (LCI) device. The sensing probe is a fiber-based Fizeau-Interferometer, which means, that the two beams, which get reflected from the fiber end surface due to Fresnel-reflection and from the object, encode the measurement distance as an optical path difference (OPD). The OPD has to be decoded in the second part of the LCI device, which is a modified Michelson-Interferometer.

The light of two pigtailed low-coherent, superluminiscent diodes (SLD) is coupled into the system with singlemode fiber couplers and is guided to the sensing probe, where it is partly emitted to the measuring object. As mentioned before, the OPD gets balanced in the Michelson-Interferometer. Therefore, the length difference between beam splitter and reference mirror and between beam splitter and tilted mirror, respectively, have to match the OPD. Instead of mechanical tuning, this problem has been solved with the so-called electronic tuning. The small tilt angle of one mirror leads to a spatial projection of a defined measuring range and the whole range is imaged on the detector, without any moving elements like piezoelectric actuators or linear stages. The measuring distance correlates with the lateral position of the characteristic interfererence pattern on the CCD-line.

The used SLDs feature two different central wavelengths $\bar{\lambda}_1$=754.2 nm and $\bar{\lambda}_2$=826.7 nm. The emerging correlogram

$$I\left(z-z_0\right)=I_0\left\{1+g\left(z-z_0\right)\cos\left[2k_0\left(z-z_0\right)+\alpha\right]\right\} \tag{1}$$

depends on the optical path difference $z-z_0$, where z_0 is the balanced working distance of the system. Eqn. (1) furthermore depends on the central wave number $k_0=2\pi/\lambda_0$ of the light source and the correlogram envelope function $g\left(z-z_0\right)$ and α, the phase-shift after reflection from the surface. In case of a light source with a gaussian spectrum, the envelope function takes the form

$$g\left(z-z_0\right)=exp\left\{-2\left[\Delta k\cdot\left(z-z_0\right)\right]^2\right\}, \tag{2}$$

where $\Delta k=2\pi/\Delta\lambda$ denotes the spectral width of the light source.[6] The maximum of the envelope can be used to determine the corresponding point of the object surface. For achieving a higher accuracy, also the phase modulation can be analyzed.[7] The accuracy and stability of the fringe pattern evaluation is influenced by the spectral properties of the light sources. The system described within this work uses SLDs with a full width at half maximum (FWHM) of $\Delta\lambda_1$ =21.7 nm and $\Delta\lambda_2$=25.3 nm. Fig. 2 shows, that the resulting correlogram shows

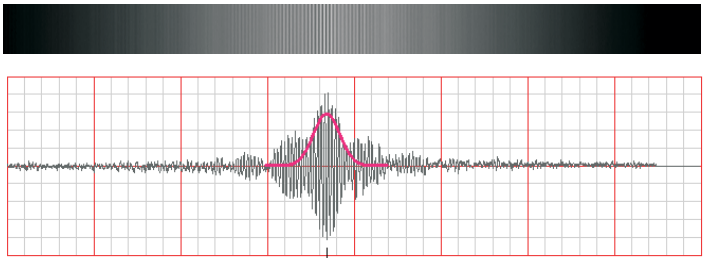

Figure 2. Correlogram with beat signal for the low-coherence interferometer with two SLDs (λ_1=754.2 nm, λ_2=826.7 nm)

an additional beat modulation of the envelope, due to the use of light sources with two different wavelengths. Thus, the central envelope peak gets sharper and the effective coherence length is reduced to

$$l_c \approx \frac{1}{2\sqrt{2\ln 2}} \frac{\bar{\lambda}_1 \bar{\lambda}_2}{\bar{\lambda}_2 - \bar{\lambda}_1} \tag{3}$$

With $\bar{\lambda}_1$ =754.2 nm and $\bar{\lambda}_2$=826.7 nm the effective coherence length for the described system is 3.6 µm. A detailed description of the system set-up and signal processing can be found in Ref. 7.

The system is capable for absolute distance measurements with a resolution of 0.1 nm and an uncertainty of $u_c = 10$ nm (k=2). Depeding on the surface quality of the specimen, measurement frequencies of 2 kHz and more are possible. The measuring range can be varied with the mirror tilt angle. For the roughness measurements, a system configuration with aprox. 140 µm has been used.

2.2 Miniaturized sensing probe

The sensing Fizeau-probe is realized as an all-fiber solution, which means, that both beam shaping and the connection to the LCI device are realized by means of optical fibers. The basic probe configuration is shown in Fig. 3a. A piece of GRIN-fiber is connected with a singlemode fiber by fusion-splicing. The realization of collimated and focussed beams are possible by the use of graded-index (GRIN) fibers, as described in Ref. 8 and Ref. 9, whereas the focal length f is affected by the length L of the GRIN-fiber with

$$f(L) = \frac{n\left(1 - \frac{w^4}{w_0^4}\right)\cos(gL)\sin(gL)}{gn_0\left[\sin^2(gL) + \frac{w^4}{w_0^4}\cos^2(gL)\right]}, \tag{4}$$

where w_0 is the waist size of the beam, that leaves the singlemode fiber, n is the refraction index of the medium, into which light beams emerge from the fiber lens (e.g. $n \approx 1$ for air). The gradient constant g and n_0 denote the

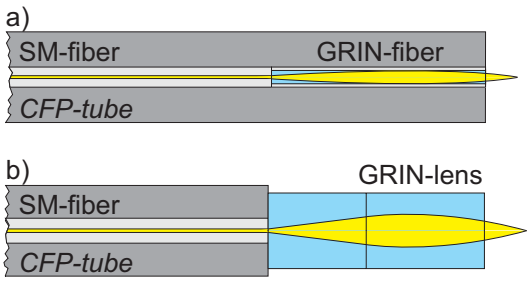

Figure 3. Basic probe configuration with (a) singlemode and GRIN-fiber, (b) singlemode fiber and GRIN-lens

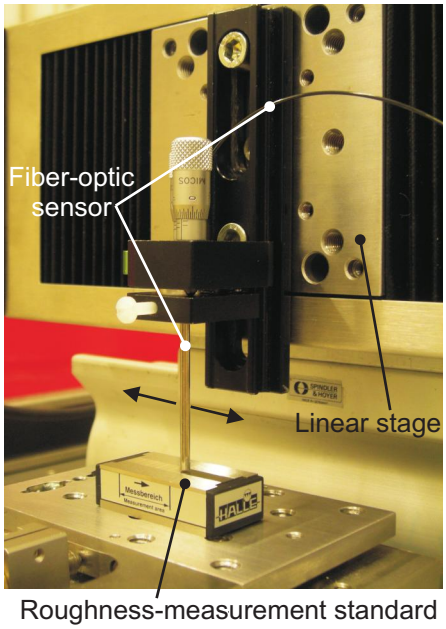

Figure 4. Set-up for roughness measurements

refraction index profile of the used GRIN fiber. The factor w depends on the wavelength λ by $w = \lambda/(\pi g n_0)$.[9] The fiber probe can be protected against fracture and environmental influences with micro-tubes of materials such as carbon fiber reinforced plastic (CFP), nitinol or other materials. In this case, the tube thickness is the limiting factor in a probe miniaturization. Today, probes with standard 250 µm fibers and nitinol tubes with diameters down to 430 µm have already been realized. Smaller probe diameters are possible by using reduced-cladding (RC) fibers with 80 µm cladding diameter or tapered fibers. Such probe designs will result in a lower numerical aperture. For high NA probes, large diameter fibers (LDF) with core diameters up to 360 µm can be used and numerical apertures of 0.2 and more can be realized.

To achieve probe designs with a high NA, GRIN-lens based set-ups can be realized. Fig. 3b shows a design with a singlemode fiber, a GRIN-lens and a glass spacer, which causes a divergence of the beam diameter from the singlemode fiber before it enters the GRIN-lens. Because of the lower refraction index for the marginal rays in the GRIN medium, a higher numerical aperture can be reached. To reduce dispersion effects, which cause a limitation of the interference contrast over the measuring range, a plano-concave focussing lens can be used as reference plane.[10]

2.2.1 Set-up for surface analysis

In order to analyze the surface parameters, the fiber-optical probe has to be moved over the surface with an accurate scanning movement. This is achieved by using a high-resolution linear stage to which the probe is attached. The measuring surface is placed over a 5-DOF table, which is capable of aligning the surface with the stage trajectory. Fig. 4 shows the setup used to perform the measurements.

The stage controller was configured to transmit a TTL trigger signal to the framegrabber on certain stage encoder positions. This procedure enables equally spaced measurements on the object surface. Evaluation length and sampling step were chosen according to ISO 3274.[11]

Is is worth to mention, that due to the microstructure of the surface under test and the limited lateral resolution of the low-coherence interferometer system, a speckle pattern arises,[12] that is superimposed with the fringe pattern and causes a longitudinal measurement uncertainty. Ref. 13 describes, that the operation of low-coherence interferometry on rough surfaces can be described in two regimes, which are divided by the limit

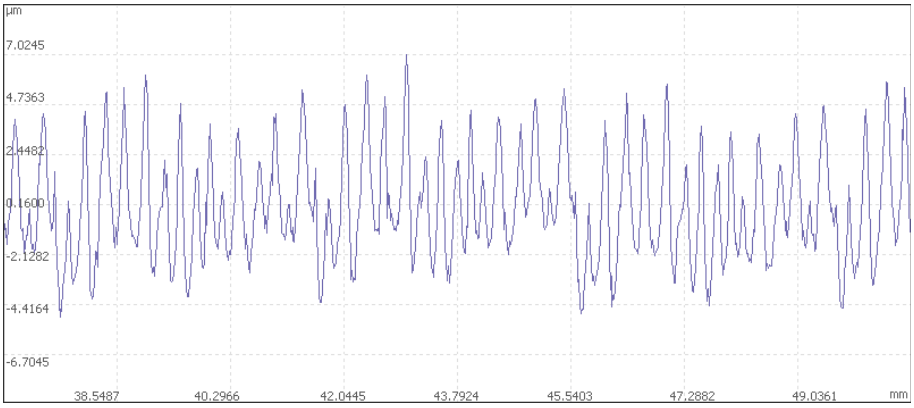

Figure 5. Measured profile of type D1 roughness-measurement standard (nominal R_a=1.82 µm)

spectral width. Besides that, the longitudinal measurement uncertainty δ_z is directly related to the surface rms roughness σ_h and does not depend on the system parameters, such as the spectral width:

$$\delta_z = \frac{1}{\sqrt{2}} \sqrt{\frac{\langle I_{obj} \rangle}{I_{obj}}} \sigma_h \tag{5}$$

I_{obj} denotes the intensity of an individual speckle on the surface. For a gaussian height distribution the rms roughness σ_h correlates to the average roughness by $R_a = 0.8 \cdot \sigma_h$.

3. EVALUATION

A series of measurements was performed to evaluate the system. Roughness-measurement standards of ISO 5436-1 types A2, D1 and D2[14] and a sine reference specimen were measured. The results were compared to the nominal values provided in their calibration certificates. Standards of those types are commonly used for the calibration of tactile stylus instruments. For the measurements a focussing probe with a 1.8 mm diameter GRIN-lens and plano-concave reference lens has been used.

In order to acquire and process measurement data, a software has been developed, which automatically determines the evaluation length, sampling step and scanning step, which is needed for a surface with specified nominal roughness, and also controls the measuring process. Furthermore the software is able to evaluate the acquired data and calculate roughness parameters according to ISO 4288[15] as well as waviness and profile parameters. To ensure an accurate calculation, the software has been calibrated with so-called software measurement standards, which are reference data files with given surface parameters.[16]

3.1 Roughness-measurement standards

The validation of the system was performed by means of measuring calibrated roughness standards. For comparison of the measurement results and the nominal values, the average roughness value R_a has been selected, which is given by

$$R_a = \frac{1}{l} \int_0^l |Z(x)| \, dx \tag{6}$$

for the sampling length l, which in case of roughness analysis, is always equal to the cut-off wavelength λ_c of the gaussian high-pass filter. $Z(x)$ is the ordinate value, which remains after the primary profile filtering, which also eliminates a possible tilt of the measurement data. Fig. 5 shows the unfiltered profile, which has been measured for the type D1 roughness-measurement standard with a nominal average roughness of R_a=1.82 nm.

Three different roughness-measurement standards of types D1 and D2 (ISO 5436-1) were measured, with nominal R_a of 1.82 µm, 0.0813 µm and 0.0226 µm. Table 1 shows the mean value for R_a for the type D standards, obtained with twenty measurements.

	Nominal value [µm]	Mean value for 20 measurements [µm]
Standard 1 (Type D1)	1.8200	1.7426
Standard 2 (Type D2)	0.0813	0.0740
Standard 3 (Type D2)	0.0226	0.0294

Table 1. Measurement results for type D roughness-measurement standards

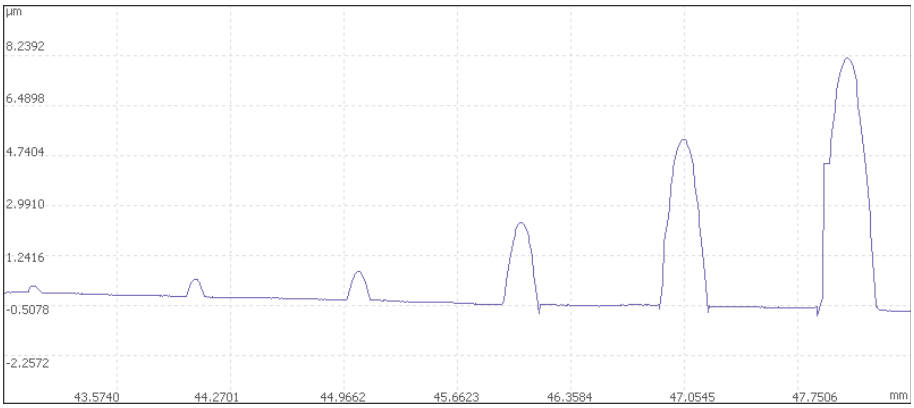

Figure 6. Measured profile of type A2 depth-setting standard with six grooves (round ground)

The results show a good correlation between the measured and nominal average roughness. Due to a spot size, which is approx. 5 µm, a slightly lower measured roughness can be expected, which is the case for the standards 1 and 2 in Table 1. The super-smooth standard 3 shows a higher measured roughness. This can be explained by a minimal noise level, which is about 2 nm. Besides that, the deviation can also be explained by the measurement uncertainty of the system.

3.2 Depth-setting standard

The system has also been evaluated by measuring six grooves of a depth-setting standard according to ISO 5436-1. The grooves had nominal depths of 0.256 µm, 0.633 µm, 1.040 µm, 2.890 µm, 5.910 µm and 8.860 µm (Fig. 6).

Table 2 shows the depth mean value for each of the six grooves in the type A2 standard, obtained with twenty measurements.

	Nominal value [µm]	Mean value for 20 measurements [µm]
Groove 1	0.256	0.250
Groove 2	0.633	0.619
Groove 3	1.040	1.003
Groove 4	2.890	2.833
Groove 5	5.910	5.812
Groove 6	8.860	8.732

Table 2. Measurement results for the type A2 standard

The results show a slight but systematic difference between measured and nominal groove depths. This can be compensated with an improved calibration, which has been done with reference to the wavelengths of the light sources. This way, a self-calibration can be achieved with the trade-off, that the overall accuracy depends on the frequency stability. At the groove edges, the measurement results show the so-called batwing artifacts, which are characteristic for low-coherence interferometry.[17]

3.3 Sine reference specimen

A sine reference specimen has also been measured with the described system. The specimen 531E by Rubert consists of a sine wave shaped surface profile with a period length of S_m=100 µm and a profile depth of P_t=1 µm. The specimen is an ISO 5436-1 Type C1 standard and represents an idealized rough surface with a nominal R_a of 0.3 µm.

Table 3 shows the mean value of five measurements for the sine wave reference specimen. The specimen could

	R_a	S_m
Mean value of 5 measurements [µm]	0.3	101
Nominal value [µm]	0.3	100

Table 3. Measurement results for the type C1 sine wave reference specimen

be measured without any missing data, even for the sloped areas of the surface.

4. CONCLUSION

Within this work, a fiber-optic low-coherence interferometer has been proposed and its applicability for surface profile analysis has been investigated. Exemplarily, the surface roughness, which is one of the most demanding measuring tasks for optical sensors, has been tested. The measurement results for various calibration standards show the potential for highly accurate, non-contact measurements even on rough surfaces.

Fields of application could be e.g. the measurement inside small boreholes such as fuel injection nozzles. In this regard, not only the roundness but also the roughness of the cylindrical wall is of interest, i.e. for the friction of the injection needle. Similar to that, also the measurement of roughness inside small fittings can be realized, since this is a functional property of such parts.

Yet, additional measurement series have to be conducted using standards with higher roughnesses in order to evaluate the limitations of fiber-optic profil analysis. Furthermore, the influence of numerical aperture on the measurement accruracy has to be studied.

5. ACKNOWLEDGEMENTS

We gratefully acknowledge the financial support by the German Ministry of Education and Science BMBF for the project 'MikroFiz' (FKZ 13N9495), which is the basis for the proposed achievements.

REFERENCES

[1] Klocke, F., Dambon, O., Sarikaya, H., Hollstege, D., and Pongs, G., "Investigation to the molding accuracy of complex shaped glass components," in [*Proceedings of the 10th anniversary international conference of the European Society for Precision Engineering and Nanotechnology: May 18th - May 22nd 2008, Zürich, Switzerland*], Brussel, H. v., ed., 2–6, Euspen, Bedford (2008).

[2] Brecher, C., Lange, S. C., Merz, M., Niehaus, F., and Winterschladen, M., "Off-axis machining of nurbs freeform surfaces by fast tool servo systems," in [*Second international conference on multi-material micro manufacture: 20-22 September 2006 Grenoble, France4M2006*], 4M Network of Excellence, ed., Elsevier, Oxford (2006).

[3] Wyant, J. C., Koliopoulos, C. L., Bhushan, B., and Basila, D., "Development of a three-dimensional non-contact digital optical profiler," *Journal of Tribology* **108**, 1–8 (1986).

[4] Jordan, H.-J., Wegner, M., and Tiziani, H., "Highly accurate non-contact characterization of engineering surfaces using confocal microscopy," *Measurement Science and Technology* **9**(7), 1142–1151 (1998).

[5] Windecker, R., Franz, S., and Tiziani, H. J., "Optical roughness measurements with fringe projection," *Appl. Opt.* **38**(13), 2837–2842 (1999).

[6] Born, M., Wolf, E., and Bhatia, A. B., [*Principles of optics: Electromagnetic theory of propagation, interference and diffraction of light*], Cambridge Univ. Press, Cambridge, 7 ed. (2006).

[7] Depiereux, F., Lehmann, P., Pfeifer, T., and Schmitt, R., "Fiber-optical sensor with miniaturized probe head and nanometer accuracy based on spatially modulated low-coherence interferogram analysis," *Appl. Opt.* **46**(17), 3425–3431 (2007).

[8] Emkey, W. and Jack, C., "Analysis and evaluation of graded-index fiber lenses," *J. Lightwave Technol.* **5**(9), 1156–1164 (1987).

[9] Reed, W. A., Yan, M. F., and Schnitzer, M. J., "Gradient-index fiber-optic microprobes for minimally invasive in vivo low-coherence interferometry," *Optics Letters* **27**(20), 1794–1796 (2002).

[10] Malacara, D., [*Optical shop testing*], Wiley, Hoboken, NJ, 3. ed. (2007).

[11] [*ISO 3274:1996: Geometrical Product Specifications (GPS) – Surface texture: Profile method – Nominal characteristics of contact (stylus) instruments*] (1996).

[12] Häusler, G., Ettl, P., Schenk, M., Bohn, G., and Laszlo, I., "Limits of optical range sensors and how to exploit them," in [*International trends in optics and photonics ICO IV*], Asakura, T., ed., 328–342, Springer, Berlin (1999).

[13] Pavliček, P. and Hýbl, O., "White-light interferometry on rough surfaces-measurement uncertainty caused by surface roughness," *Appl. Opt.* **47**(16), 2941–2949 (2008).

[14] [*ISO 5436-1:2000: Geometrical Product Specifications (GPS) – Surface texture: Profile method; Measurement standards – Part 1: Material measures*] (2000).

[15] [*ISO 4288:1996: Geometrical Product Specifications (GPS) – Surface texture: Profile method – Rules and procedures for the assessment of surface texture*] (1996).

[16] [*ISO 5436-2:2001: Geometrical Product Specifications (GPS) – Surface texture: Profile method; Measurement standards – Part 2: Software measurement standards*] (2001).

[17] Harasaki, A. and Wyant, J. C., "Fringe modulation skewing effect in white-light vertical scanning interferometry," *Appl. Opt.* **39**(13), 2101–2106 (2000).